

Rational design of guiding elements for control over folding topology in i-motifs with multiple quadruplexes

Alexander S. Minasyan,^a Srinivas Chakravarthy,^b Suchitra Vardelly,^a Mark Joseph,^c

Evgeni E. Nesterov,^a and Irina V. Nesterova^{a,*}

^a Department of Chemistry and Biochemistry, Northern Illinois University, DeKalb, IL 60115, USA

^b X-ray Science Division, Argonne National Laboratory, Argonne, IL 60439, USA

^c Department of Natural Science, University of Maryland Eastern Shore, Princess Anne, MD 21853, USA

SUPPORTING INFORMATION

TABLE OF CONTENTS

MATERIALS AND METHODS.....	S2
Reagents.....	S2
pH: adjusting and measuring	S2
Sample preparation	S2
Thermal denaturation studies by UV spectroscopy	S2
pH Denaturation studies by UV spectroscopy	S4
SEC/SAXS experiments	S4
SAXS data processing.....	S4
DETAILED DESCRIPTION OF SEC/SAXS EXPERIMENTS.....	S5
SUPPLEMENTARY FIGURES.....	S6
Figure S1.....	S6
Figure S2.....	S7
Figure S3.....	S7
Figure S4.....	S7
Figure S5.....	S8
Figure S6.....	S8
Figure S7.....	S9
Figure S8.....	S9
Supplementary table.....	S10
Table S1.....	S10
REFERENCES TO SUPPORTING INFORMATION.....	S11

MATERIALS AND METHODS

Reagents

All chemical reagents were obtained from established commercial suppliers (i.e. Sigma-Aldrich (St. Louis, MO), Fisher Scientific (Pittsburg, PA), and others). Single stranded DNAs were obtained from IDT (Coralville, IA). Oligonucleotide sequences are included in Figure 1 (main text). Nuclease-free water for preparation of DNA solutions was obtained from IDT (Coralville, IA). PBS buffer (0.01 M Na₂HPO₄, 0.0018 M KH₂PO₄, 0.137 M NaCl, 0.0027M KCl) and lithium cacodylate buffer (10 mM) were prepared in house. Oligonucleotide sequences are included in Figure 1. pH-meter calibration buffers (4.00 ± 0.01, 7.00 ± 0.01, and 10.00 ± 0.02) were purchased from Fisher.

pH: adjusting and measuring

Thorough control over pH is crucial for reliable conclusions on i-motifs transitions. ThermoOrion pH-meter (Model 420) was used throughout the studies. The pH meter was calibrated every time used against fresh aliquots of pH calibration buffers. The pH meter accuracy was confirmed over the calibration range against pH calibration buffers and never exceeded buffer's nominal value ± 0.02 units. pH values of PBS buffers were adjusted with H₃PO₄ and/or NaOH; pH values of Lithium cacodylate buffers were adjusted with cacodylic acid and/or LiOH. Actual pH values were used to plot graphs in Figure 2b (main text).

Sample preparation

Oligonucleotides obtained from IDT were reconstituted with nuclease free water to yield 100 - 700 μM stock solutions.

A typical sample for pH denaturation studies (1000 μL) was prepared by diluting an oligonucleotide stock solution to a concentration of 500 nM with PBS buffer of an appropriate pH, heating the solution at 95°C for 15 minutes followed by slow (overnight) cooling to room temperature. Every sample was prepared and analysed in triplicate.

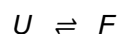
A typical sample for SEC/SAXS (800 μL) was prepared by diluting an oligonucleotide stock solution to a concentration of 50 μM with a PBS buffer of an appropriate pH, heating the solution at 95°C for 15 minutes followed by slow (overnight) cooling to room temperature.

Thermal denaturation studies by UV spectroscopy

Thermal denaturation studies via UV spectroscopy (Figures 2a (main text) and S2) were performed using a Cary 4000 UV-Vis spectrophotometer (Agilent Technologies, Santa Clara, CA). Typically, measurements were performed on a 800-μL aliquot of a 200 nM sample using a 10 mm optical path cuvette. The i-motif transitions were monitored at 295 nm where C-quadruplex unfolding is accompanied by the hypochromic effect.¹⁻³ The denaturations were acquired in 10 mM Li cacodylate as a buffer with negligible effect of temperature on pH.⁴

First, the oligonucleotide samples were denatured at 80 °C for 30 min in cuvettes inside a sample compartment of a spectrometer. Then the samples were cooled at 0.2 °C min⁻¹ rate to 8 °C. Absorption spectra was acquired at each temperature. Upon completion of the cooling cycle, samples were stored overnight at 5 °C. Next morning the samples were equilibrated at 8 °C for 30 min inside a sample compartment of UV-vis spectrometer before the heating cycle. The samples were heated at 0.2 °C min⁻¹ rate to 60 °C; absorption spectra were collected at each temperature.

All the thermal denaturation profiles yielded hysteresis loops (Figures 2a and S2). To derive k_f 's and k_u 's we used an approach reported earlier⁵ modified to suit intramolecular folds. Briefly, for unfolded quadruplex (U) to folded (F) transition



the rate equation is

$$\frac{d[F]}{dt} = -\frac{d[U]}{dt} = -k_f^T[U] + k_u^T[F] \quad (\text{eq.1})$$

Where

[F] concentration of folded i-motif

[U] concentration of unfolded i-motif

k_f^T folding rate constant (at temperature T)

k_u^T unfolding rate constant (at temperature T)

Assuming that α is a fraction of folded i-motif ($\alpha = \frac{[F]}{[F]+[U]}$) and $(1 - \alpha)$ is a fraction of unfolded i-motif ($1 - \alpha = \frac{[U]}{[F]+[U]}$), eq.1 can be transformed:

$$\frac{d[\alpha]}{dt} = -k_f^T[1-\alpha] + k_u^T[\alpha] \quad (\text{eq.2})$$

Applying the equation 2 for a typical hysteresis cycle (e.g. Fig. 2A and S2), yields the following system:

$$\text{Cooling curve: } \frac{d\alpha_c}{dT} = \left(\frac{dT}{dt}\right)_c^{-1} [k_f^T(1 - \alpha_c) - k_u^T \alpha_c] \quad (\text{eq. 3})$$

$$\text{Heating curve: } \frac{d\alpha_h}{dT} = \left(\frac{dT}{dt}\right)_h^{-1} [k_f^T(1 - \alpha_h) - k_u^T \alpha_h] \quad (\text{eq.4})$$

where

α_c fraction of folded i-motif deduced from cooling cycle

α_h fraction of folded i-motif deduced from heating cycle

Solving the system of two linear equations 3 and 4 at each temperature yields values of k_f^T and k_u^T used to plot graphs in Figures S3 and S4.

Equilibrium melting temperatures (T_m 's) were derived from Arrhenius plots (Figures S3 and S4 for pH 6.80 and 6.70, respectively).

Equilibrium constants (K_{eq}) at each temperature were determined as k_f/k_u . Values of $\ln(K_{eq})$ were plotted as a function of $1/T$ (T is temperature). Linear fits of the data were utilized to derive values of ΔH° and ΔS° using standard van't Hoff analysis.

pH Denaturation studies by UV spectroscopy

pH Denaturation studies via UV spectroscopy were performed using a Cary 4000 UV-Vis spectrophotometer (Agilent Technologies, Santa Clara, CA). Typically, measurements were performed on a 800- μ L aliquot of a 500 nM sample in PBS buffer of an appropriate pH using a 10 mm optical path cuvette. The samples were denatured at 95 °C for 10 min and cooled to a room temperature overnight. The i-motif transitions were monitored at 295 nm where C-quadruplex unfolding is accompanied by the hypochromic effect.¹ All the measurements were taken at room temperature.

SEC/SAXS experiments

Detailed conditions for SEC/SAXS experiments are summarized below. Briefly, size exclusion chromatography (SEC) combined with small-angle X-ray scattering (SAXS) studies were conducted at BioCAT (beamline 18-ID) facility at Advanced Photon Source in Argonne National Lab (Lemont, IL, USA). The upfront separation was conducted using Superdex 75 (MW ~3-70 kDa) column (GE Healthcare, Chicago, IL, USA) which was run at a flow rate of 0.7 mL min⁻¹. PBS buffer at the same pH as analysed sample was used as a mobile phase for SEC separation. Immediately after the separation column, the eluate ran through UV-vis detector where absorption at 260 nm was monitored (Figure 3). After passing through the UV-vis detector, the eluate was flowed through a SAXS flow cell, which consisted of a 1 mm ID quartz capillary with ~50 μ m walls. A coflowing buffer sheath was used to separate sample from the capillary walls, helping prevent radiation damage.⁶ Scattering intensity was recorded using a Pilatus3 1M detector (Dectris Ltd., Switzerland) which was placed ~3.5 m from the sample resulting in a q -range of ~0.0043 to 0.35 \AA^{-1} . Exposures of 0.5 s were acquired every 2 s during elution. Buffer blanks were created by averaging regions flanking the elution peak and subtracted from exposures selected from the elution peak to create $I(q)$ vs. q curves used in further analyses.

SAXS data processing

The raw SAXS data were reduced using BioXTAS RAW 1.6.3 software.⁷ Pair distance distribution function $P(r)$ was obtained from scattering data using GNOM software⁸ as implemented in ATSAS package.⁹ Reconstruction of the electron density surfaces from scattering data was carried out using DENSS algorithm¹⁰ as implemented in BioXTAS RAW software. The electron density maps were plotted using PyMOL software.¹¹

DETAILED DESCRIPTION OF SEC/SAXS EXPERIMENTS

SEC/SAXS data collection parameters	
Instrument	BioCAT facility at the Advanced Photon Source, beamline 18ID with Pilatus3 1M (Dectris) detector
Wavelength (Å)	1.033
Beam size (μm ²)	~ 150 (h) x 100 (v)
Camera length (m)	3.673
q -measurement range (Å ⁻¹)	0.0043-0.35
Absolute scaling method	N/A
Basis for normalization to constant counts	To transmitted intensity measured by active beam stop
Method for monitoring radiation damage	Automated frame-by-frame comparison of relevant regions
Exposure time, number of exposures	0.5 s exposure time with a 2 s total exposure period (0.5 s on, 1.5 s off) of entire SEC elution
Sample configuration	SEC-SAXS. Size separation by an AKTA Pure with a Superdex 75 10/300 GL column. SAXS data measured in a Coflow sample cell.
Sample temperature (°C)	22
Software employed for SAS data reduction, analysis and interpretation	
SAXS data reduction	Radial averaging; frame comparison, averaging, and subtraction done using BioXTAS RAW 1.6.3 ⁷
Basic analysis: Guinier, M.W., $P(r)$	Guinier fit and molecular weight using BioXTAS RAW 1.6.3, $P(r)$ function using GNOM ⁸

SUPPLEMENTARY FIGURES

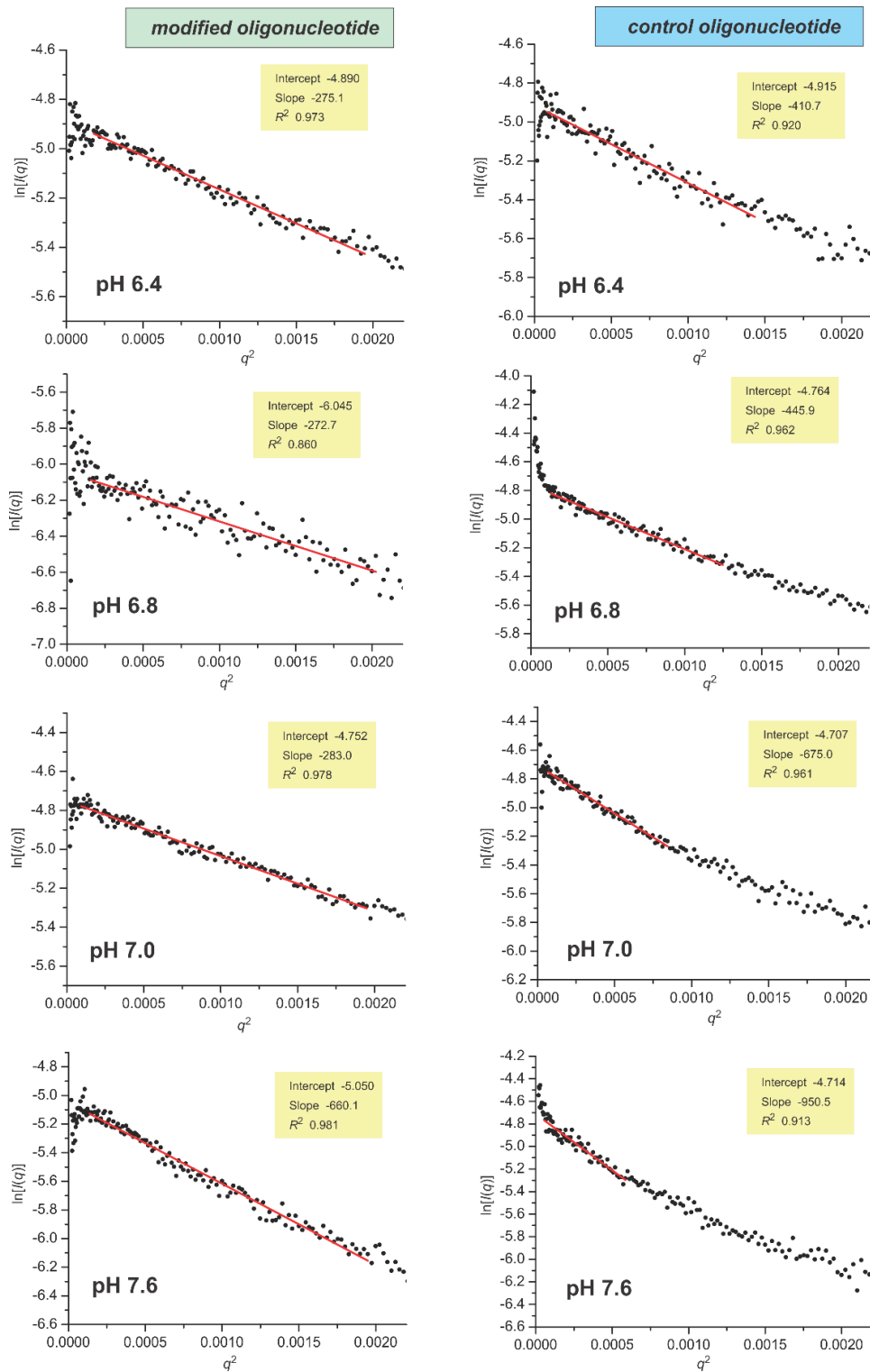


Figure S1. Guinier plots for the scattering data in Figure 4(A, B), and corresponding linear fits used to determine R_g values. Left column: data for the modified oligonucleotide, right column: data for the control.

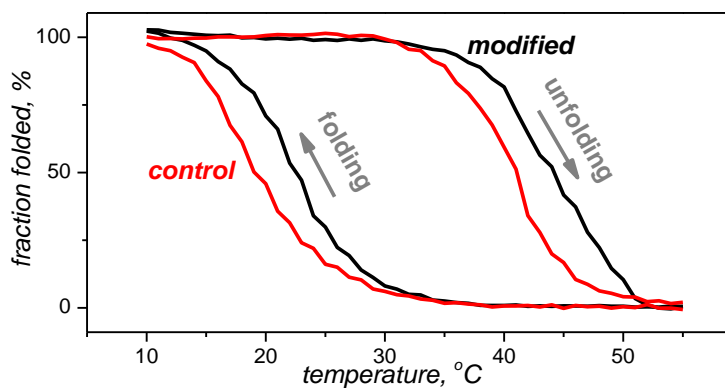


Figure S2. Thermal folding/unfolding profiles for modified (black) and control (red) i-motifs in 10 mM Lithium cacodylate (pH 6.70) buffer at 0.2 °C min⁻¹ cooling/heating rate.

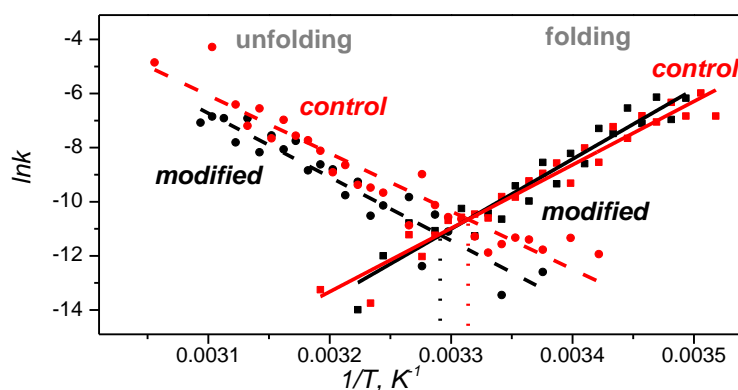


Figure S3. Arrhenius plots of folding (k_f , squares, solid line fits) and unfolding (k_u , circles, dashed line fits) rates for modified (black) and control (red) i-motifs. Positions of fits intersections ($k_f = k_u$, dotted dropout lines) indicate to equilibrium melting temperatures (T_m 's). The data were acquired at pH 6.80.

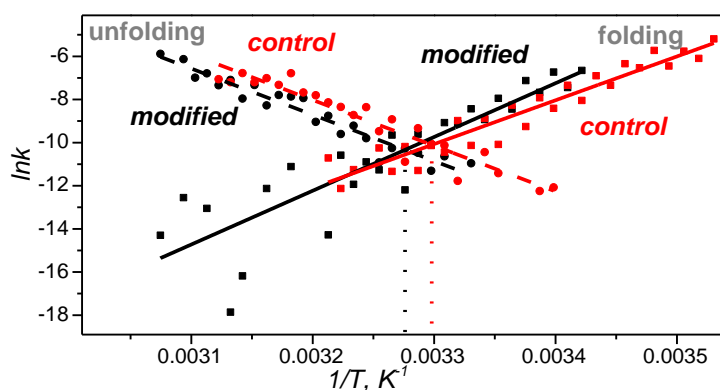


Figure S4. Arrhenius plots of folding (k_f , squares, solid line fits) and unfolding (k_u , circles, dashed line fits) rates for modified (black) and control (red) i-motifs. Positions of fits intersections ($k_f = k_u$, dotted dropout lines) indicate to equilibrium melting temperatures (T_m 's). The data were acquired at pH 6.70.

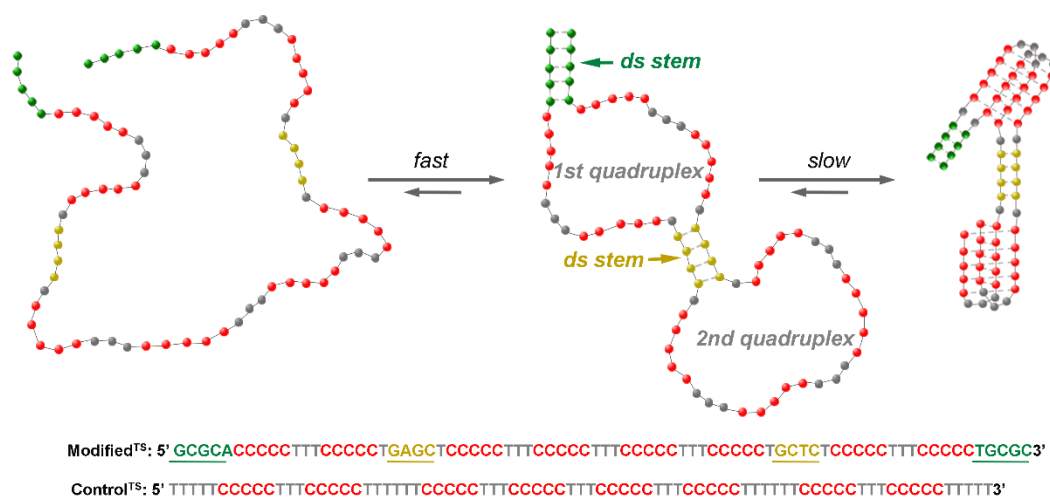


Figure S5. Folding pathways for i-motif with two quadruplexes defined by two stems (TS) An oligonucleotide strand with eight runs of cytosines (red) modified with two guiding double stranded stems - internal (yellow) and external (green) – folds into two discrete quadruplexes in a dumbbell pattern. A control strand that is not modified with the guiding stems. Bases participating in the formation of stems are underlined, neutral thymidines are grey, cytosines – red.

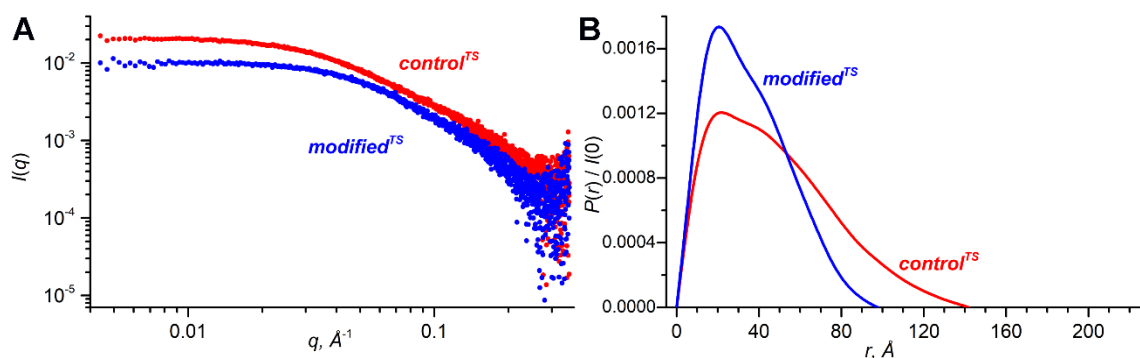


Figure S6. (A) Original scattering data ($I(q)$ vs. q) and (B) normalized pair distance distribution function ($P(r)/I(0)$) derived from the scattering data clearly indicates more compact shape of the modified oligonucleotide (red) compared to the control (blue).

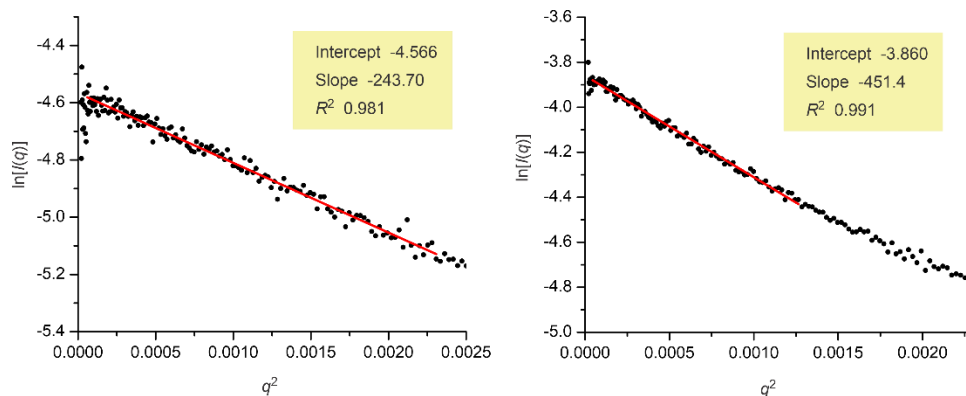


Figure S7. Guinier plots for scattering data in Figure S6, and corresponding linear fits used to determine R_g values. Left graph: data for the new modified oligonucleotide, right graph: data for the control.

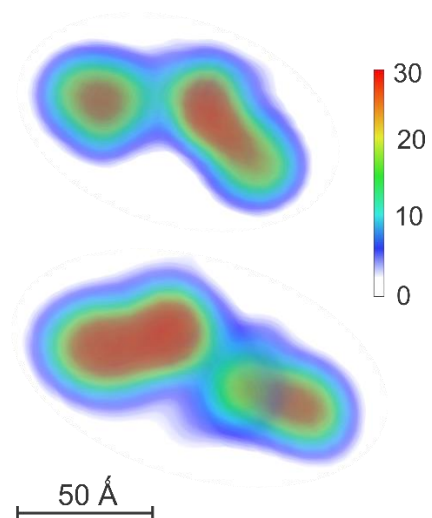


Figure S8. . Electron density reconstruction of the folded conformations of the new modified (top) and control (bottom) oligonucleotides in solution at pH 6.7. The maps were obtained using the DENSS algorithm based on the corresponding experimental scattering data, the electron densities are shown as volumes colored according to density (a color bar indicates electron density in the units of σ). The estimated resolution for the reconstructions is 24 Å for the new modified and 30 Å for the control oligonucleotide.

Supplementary table

Table S1. Values for R_g and D_{max} derived from $P(r)$ function analysis and, independently, from analysis of the Guinier plots.

pH	$R_g, \text{ \AA}$				$D_{max}, \text{ \AA}$	
	Modified ^{TS}		Control ^{TS}		Modified ^{TS}	Control ^{TS}
	$P(r)$ analysis	Guinier plot	$P(r)$ analysis	Guinier plot	$P(r)$ analysis	$P(r)$ analysis
6.7	28.3	27.2	39.1	36.7	98	142

REFERENCES TO SUPPORTING INFORMATION

- 1 J. L. Mergny and L. Lacroix, *Nucleic Acids Res.*, 1998, **26**, 4797.
- 2 J. L. Mergny and L. Lacroix, *Oligonucleotides*, 2003, **13**, 515.
- 3 P. A. Rachwal and K. R. Fox, *Methods*, 2007, **43**, 291.
- 4 H. Fukada and K. Takahashi, *Proteins: Struct., Funct., Genet.*, 1998, **33**, 159.
- 5 M. Rougée, B. Faucon, J. L. Mergny, F. Barcelo, C. Giovannangeli, T. Garestier and C. Hélène, *Biochemistry*, 1992, **31**, 9269.
- 6 N. Kirby, N. Cowieson, A. M. Hawley, S. T. Mudie, D. J. McGillivray, M. Kusel, V. Samardzic-Boban and T. M. Ryan, *Acta Crystallogr., Sect. D: Struct. Biol.*, 2016, **72**, 1254.
- 7 J. B. Hopkins, R. E. Gillilan and S. Skou, *J. Appl. Crystallogr.*, 2017, **50**, 1545.
- 8 D. I. Svergun, *J. Appl. Crystallogr.*, 1992, **25**, 495.
- 9 K. Manalastas-Cantos, P. V. Konarev, N. R. Hajizadeh, A. G. Kikhney, M. V. Petoukhov, D. S. Molodenskiy, A. Panjkovich, H. D. T. Mertens, A. Gruzinov, C. Borges, C. M. Jeffries, D. I. Svergun and D. Franke, *J. Appl. Cryst.*, 2021, **54**, doi:10.1107/S1600576720013412.
- 10 T. D. Grant, *Nat. Methods*, 2018, **15**, 191.
- 11 E. F. Pettersen, T. D. Goddard, C. C. Huang, G. S. Couch, D. M. Greenblatt, E. C. Meng and T. E. Ferrin, *J. Comput. Chem.*, 2004, **25**, 1605.